

Challenge of Water Saturation in Low Resistivity Cretaceous Reservoirs

Bitā Arbab

Senior Petro physicist and Specialist in Low Resistivity Pay at Iran. co, Irani.company, Oil company, Iran

*Corresponding author

Bitā Arbab, Senior Petro physicist and Specialist in Low Resistivity Pay at Iran.co, Irani.company, Oil company, Iran, E-mail: bitaarbab@yahoo.com

Submitted: 13 Aug 2018; Accepted: 04 Sep 2018; Published: 26 Sep 2018

Abstract

This study presents causes and reasons for lowering resistivity logs in carbonate deposit. Moreover this abstract elucidate methods for relieving of challenge water saturation estimation in cretaceous carbonate deposits with Low Resistivity Pay, in Persian Gulf. Reservoirs in the Cretaceous like Zubair, Buwaib, Shuaiba and Khatiyah formations of Southern fields have been analyzed as low resistivity carbonate. Resistivity responses reach less than 6 and even less than 1 ohm.m. Significant hydrocarbon accumulations are “hidden” these Pay zone, (LRPZ). Experimental analysis shows that reservoirs contain clay-coated grains of Lithocodium algal and is along with Micritization, Pyritization of diagenetic process are reasons for effect on resistivity response. On the other side Smectite and Kaolinite of main clays types have high CEC and greater impact on lowering resistivity. Lønøy method applied to address pore throat sizes which contain Inter crystalline porosity, Chalky Limestone, Mudstone micro porosity. NMR (Nuclear magnetic resonance and Pulse Neutron-Neutron logs have been used to modify the calculated water saturation of the wells. The study shows that reduced specific resistivity is due to texture change and presence of microscopic porosity. For defining reliable water saturation, Core NMR and Log NMR results have been used. NMR results explain that decreasing of resistivity in pay zone is related to texture and grain size variation not being existence of moved water. Irreducible water for the reservoirs is estimated between 30 to 50 %. Low resistivity zone related to microspores with less than 3 micron. Variable T2 cut off is allows to choice suitable T2 cut off values to differentiate movable from bound fluids adapted for the specific carbonate rock. T2 cut off varies between 45 to 110ms. The proper T2 cut off for these formations are extremely crucial to being able to estimate permeability and water saturation.

Introduction

Remarkable hydrocarbon accumulations are “hidden” in the reservoir intervals with low resistivity characteristics, which known as Low Resistivity Pay Zones (LRPZs). The LRPZ reservoir were first discovered in a sandstone reservoir within the Gulf of Mexico and then in carbonate layers [1,2]. These zones are commonly identified with high water saturation based on interpretation of resistivity logs which makes such intervals of low interest to exploration and perforation. LRPZ take place and have reported from both clastic and carbonate reservoirs, in carbonates. It has been reported to be as a result of either or a combination of deep high saline mud invasion, presence of conductive minerals, presence of microporosity, and anisotropic effect due to drilling high angle wells within reservoirs [3,4]. Typically, LRP zones are characterized by formation interval, with moderate to high porosities, showing extremely low resistivity less than 1 ohm meter. Evaluating aspect of LRPZ is crucial because it is a hinder for many log analyses to define reliable water saturation. In hydrocarbon carbonate reservoirs, due to the influence of diagenetic processes, it is important to know the type of pore and pore distribution. For this study, with considering on low resistivity formations, due to having comprehensive data, Dariyan formation were selected for detailed studied.

Geology and location of the region

In Persian Gulf region the Cretaceous succession is normally divided into three distinct parts. At the beginning of the Cretaceous global

sea level was relatively high and consequently, most of the Basin accumulated almost exclusively shallow-marine carbonates of Tamama group (Fig 1). The Zubair carbonate (lithostratigraphic equivalents of Gadvan Formation) is considered to have good reservoir potential in the Persian Gulf. This formation is one of the subordinate reservoir rocks in the Persian Gulf Basin. Buwaib Formation is characterized by inter-bedded porous carbonate and tight argillaceous limestones or marls. The Aptian carbonates Shuaiba Formation) forms prolific reservoirs in the eastern Persian Gulf, particularly in the UAE. During the middle Cretaceous in late Albian –Cenomanian time the khatiyah (Sarvak of Iran) inter shelf basin formed in the southern part of Persian Gulf. The khatiyah consisted of calcareous shales grading upward into argillaceous pelagic lime mudstone with abundant calcisphere and planktonic foraminifera. The borders of the continental shelf of Iran have been selected Reshadat, Salman and Soroosh Fields. Dariyan Formation was selected for detailed study. During the Middle Aptian, a large carbonate plateau is deposited in a peloidbioclastic limestone which develops in an intrashelf basin with deeper waters in the south and north of the Persian Gulf (Geological Report of the Company Off shore oil (2006). In these deep water masses, carbonaceous clays (rock origin) are deposited. By increasing the relative surface of seas in Aptian, a large carbonate platform (Dariyan / Shuaiba) expands. In the former Albian, the sea level has fallen, and in the relatively deeper basins of the Kazdumi, Nahrumr, part of the sandstone basin has been deposited from the limestone deposits of Sarvak

or Madudd. Stratigraphic sequences, formations in the upper and lower parts of the Shuiba Formation in the Persian Gulf and Arab countries are shown in Fig. 1.

Period	Epoch	Group	Formation / Member(Qatar)	Description	Formation / Member(Iran)
CRETACEOUS	Upper	Aruma Group	Shargi	Chalky Limestone, Marl	Gurpi
			Hakul	Limestone	Ilam
			Laffan	Shale	
	Middle	Waisa Group	Kahtiyah	Limestone	Sarvak
			Ahmadi	Shale	
			Maddud	Limestone	
			Nahr Umr	Shale	
	Lower	Tamama Group	Shuaiba	Limestone	Dariyan
			Zubair	Limestone, Shale	Gadvan
			Upper Buwaib	Limestone	Upper Fahliyan
Lower Buwaib			Limestone		
Yamama			Limestone		
Sulayl	Limestone, Marl	Fahliyan			

Figure 1: Stratigraphy and determination of the upper and lower boundary of Studied Formation in the Persian Gulf and Arab countries [5].

Methodology

In this study, wells in the south-east of the Persian Gulf are used to analyze microfacies and determine the rock fabric properties. This current study is based on geological reports, thin sections, routine and special cortical analysis results, and advanced petrophysical charts. In this study, the results of core and log nuclear magnetic resonance (NMR-Nuclear Magnetic Resonance) have also been used. In the description and interpretation of microfacies and fabric of rocks from 300 thin sections painted with alizarin red, the results of routine and special cortical analysis have been used. The name of the microfacies is based on the classification [8]. The study of the Fabric of Limestones by the method of is used to determine the system of pores (Pore system) [3]. Core polished samples and CT scan analysis are also used to describe microfacies.

Descriptions and Interpretations of the Facies of the Shuiba Formation

Laboratory investigations have led to defining 8 microfacies. The investigated microfacies include Mudstone and Packston Bioclast, Lithocodium Packston and Floatston which often have microscopic porosity. Micritic matrix is often developed in algae microfacies, algae Bundstone with an abundance of Lithocodium algae. The presence of coating grains, the processes of micritization and boring in samples are common. The Shuiba Formation. Which includes 1- Pelagic Foram Wackestone 2- Pelagic Gastropoda Wackestone 3- Bioclastic Wacke / Mudstone 4- Bioclastic, Orbitolina Wacke / Mudstone 5- Foram, Lithocodium Floatston 6- Lithocodium boundstone 7- Intraclast, Foram Wacke / Packstone -8- Mixed bioclast wack / Packstone. Diagenetic processes can also be such as Micritization, Pyritization, Cementation, mechanical and chemical Compaction, Neomorphism, Dissolution, Dolomitization. Due to the variation of facies and the absence of Reef dams, the sedimentary environment model of the carbonate ramp platform is considered as the Homoclinal type (HR) for the studied rock deposits. Microfacies have been identified in the internal, middle and outer ramp section. Porosity systems are more than microscopic porosity, intergranular, intergranular, and crystalline. The presence of microscopic porosity in the microfacies in the form of equant porosity, whose average

diameter is less than 1.16 mm, is one of the important factors in the reduction of specific resistivity. Which, this reservoir results in a decrease in the resistivity of between 6 and 1 ohm. Effective diagenesis processes such as micritization, pyritization in the specimens are effective in reducing the specific resistance of the reservoir. Based on the analysis of microfacies on hydrocarbon deposits with low resistivity, due to the changes in the facies and the absence of Reef dams, the sedimentary environment model of the carbonate ramp platform is considered as Homoclinal for the rock deposits studied by the Dariyan Formation. Fig 2 presents polished samples of 8 facies of the Shuiba Formation, which are well characterized by texture, boring, bioturbation, and Lithocodium texture. Figs 3 and 4 show Core photos and photomicrographs of studied facies. Fig5 illustrates Homoclinal sedimentary model based on laboratory studies and microfacial changes.

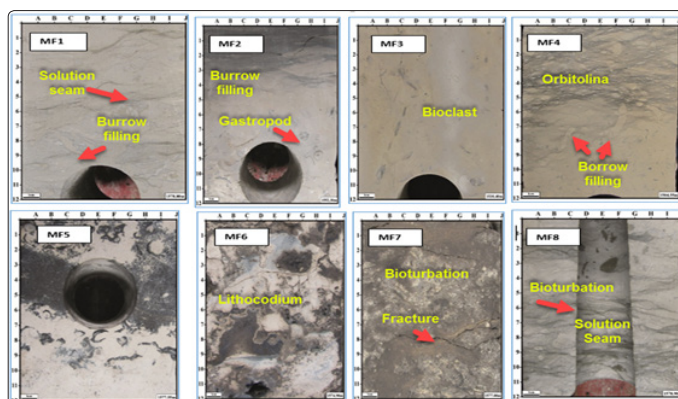


Figure 2: Polished samples have been shown in the facies of the Shuiba Formation, which are well characterized by texture, boring, bioturbation, and fractures

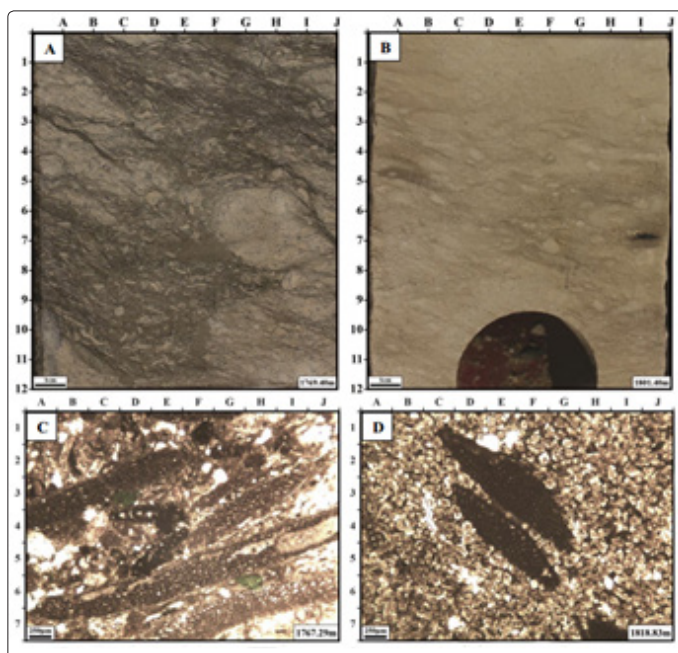


Figure 3: Core photos and photomicrographs of Bioclastic, orbitolina wacke/mudstone, Zubair, and Dariyan (Shuiba) Salman Field. A and B: Orbitolina (A) and Bioturbation (B) in the cores C and D: Glauconite (C, 6H) and Orbitolina foraminifers in the dolomitized matrix Formation

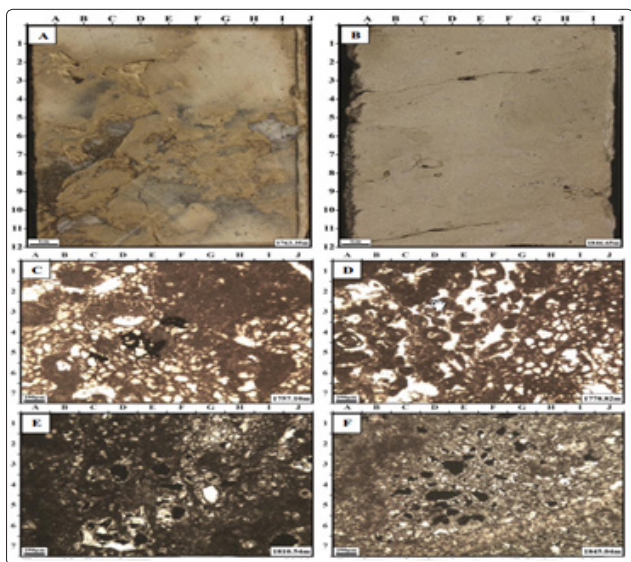


Figure 4: Core photos and photomicrographs of Lithocodium bound/float/wackestone in the Dariyan (Shuaiba) formations, Salman Field. A: Large lithocodium fragments (A, 11H) in the core samples, Dariyan (Shuaiba) Fm. B: Porous nature of this facies in slabbed core face, Shuaiba Fm.; C and D: Lithocodium talus in the thin section microphotographs and E and F: Intrafossil pores in the lithocodium fragments

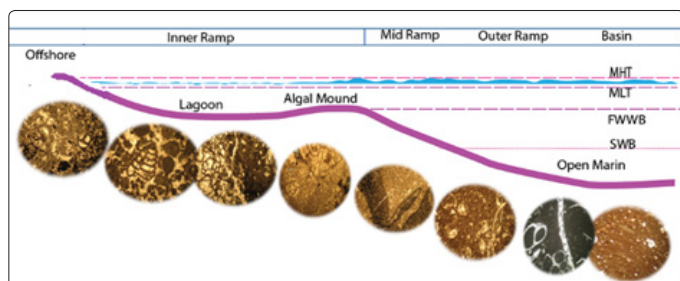


Figure 5: a Hemoclinal sedimentary model based on laboratory studies and micro facial changes

Fabric study

Since most microfacies can be varied due to various diagenetic processes and flow characteristics, finding the correct relationship between porosity and permeability is one of the important issues in the evaluation of carbonate reservoirs. In this regard, presents models that describe the importance of porosity distribution, pore size, and pore types in the classification of pore system porosity systems [6]. Most of the samples in Class 3 of Lucia are in the range of mud dominated limestones (Fig. 6). Carbonate samples of the formation, three types of pore systems, such as intercrystalline, intraparticle and microporosity, have been identified. The texture does not follow the models of the porosity system of macro and macro-crystalline porosity and does not follow the classification of one and two Lucia Figs 6 and 7. The porosity of the Mudstone microporosity system was investigated, which is ultrafine porosity of several micrometers. Mud stones with a finer porosity, between the grains of planktonic calcareous algae or between the mud particles affected by washing or burial diagenesis. Table 1 illustrates, determination the pore sizes in order of macro, micro, mesopore and rock system according to the classification and [6,7]. According to the scattering of the data, porosity and permeability are also followed by a chalky Cretaceous

lime system according to the Lønøy method (Fig. 7 and Fig 8). Mudstones with a fine porosity between the grains of calcareous algae or between the mud particles affected by washing or diagenetic burial. Based on core analysis studies using Mercury injection (Mercury Injection Capillary Pressure), samples often have a pore size of fewer than 3 microns in Fig 9. The results of experiments on capillary pressure on the studied well of core samples. The minimum non-decreasing water saturation rate is based on these capillary pressure data is 20% Fig10.

The SEM analysis on the Shuaiba sample is shown that the calcite crystals of the sample are in the form of a rhombus with small crystalline porosity and an average size of about 3 microns, Fig11.

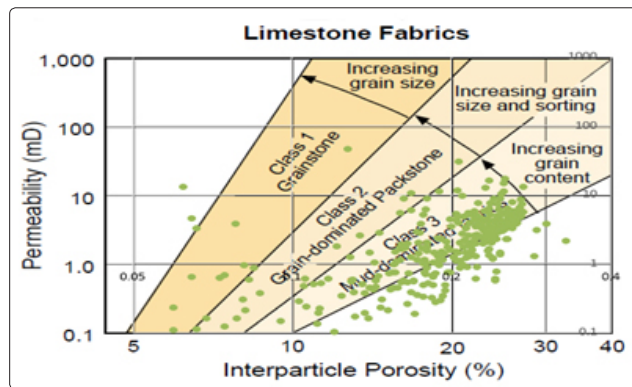


Figure 6: According to the scattering of the data, porosity and permeability of an Aptian limestone system follow the class mud dominated at class 3 Lucia

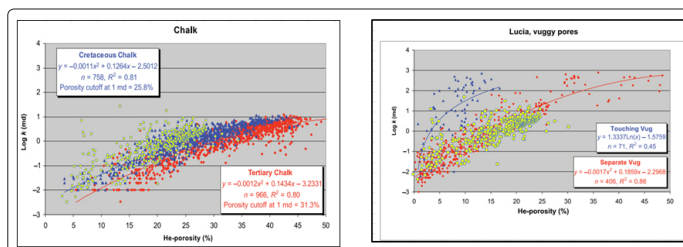


Figure 7: Pore deposition systems of Shuaiba Formation follow the model of defined Cretaceous chalk, separate Vugs, and mudstone microporosity in class 3 Lucia

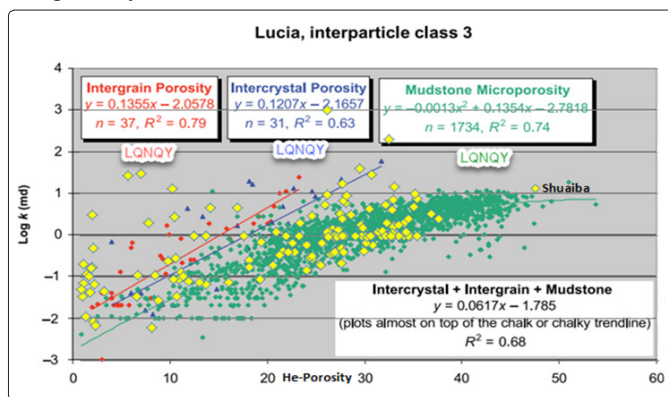


Figure 8: Pore systems of Shuaiba Formation . Yellow data shows Mudstone Microporosity

Pore Type	Pore Size	Pore Distribution	Pore Fabric
Interparticle	Micropores (10–50 μm)	Uniform	Interparticle, uniform micropores
	Mesopores (50–100 μm)	Patchy	Interparticle, patchy micropores
	Macropores (>100 μm)	Uniform	Interparticle, uniform macropores
Intercrystalline	Micropores (10–20 μm)	Patchy	Interparticle, patchy macropores
	Mesopores (20–60 μm)	Uniform	Intercrystalline, uniform micropores
	Macropores (>60 μm)	Patchy	Intercrystalline, patchy micropores
Intraparticle	Micropores (<10–20 μm)	Uniform	Intercrystalline, uniform mesopores
	Mesopores (20–60 μm)	Patchy	Intercrystalline, patchy mesopores
	Macropores (>60 μm)	Uniform	Intercrystalline, uniform macropores
Moldic	Micropores (<10–20 μm)	Patchy	Intercrystalline, patchy macropores
Moldic	Macropores (>20–30 μm)	Uniform	Intraparticle
Vuggy			Moldic micropores
Mudstone microporosity	Micropores (<10 μm)		Moldic macropores
			Vuggy
			Tertiary chalk
			Creaceous chalk
		Uniform	Chalky micropores, uniform
		Patchy	Chalky micropores, patchy

Table 1: Determine the pore size and rock system according to the classification and Lucia 1999 [6,7]

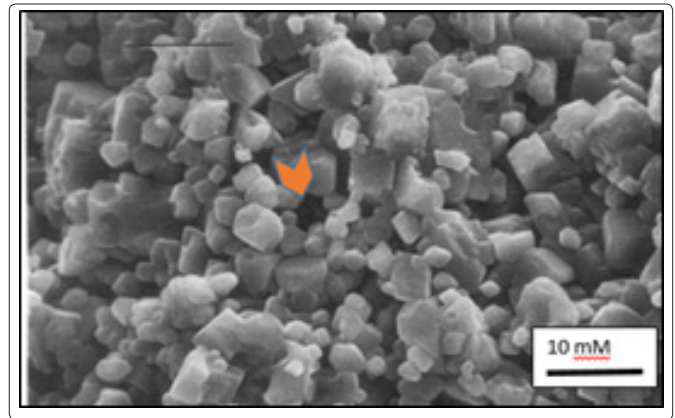


Figure 11: The SEM analysis on the Shuaiba sample is shown that the calcite crystals of the sample are in the form of a rhombus with small crystalline porosity and an average size of about 3 microns

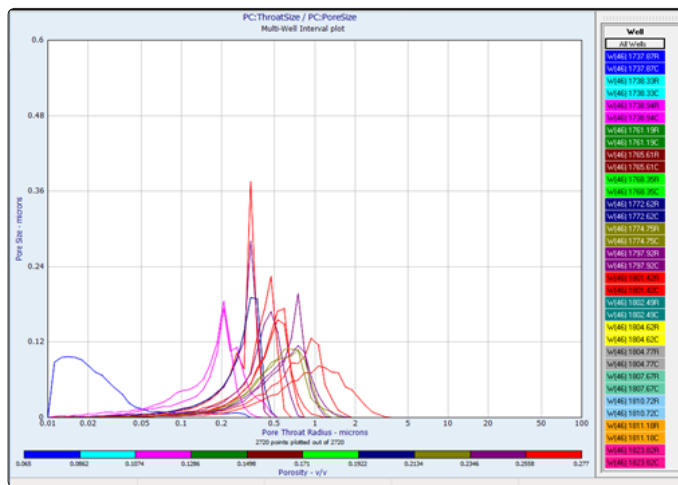


Figure 9: MICP data show that the size of the pore throat radii less than three microns

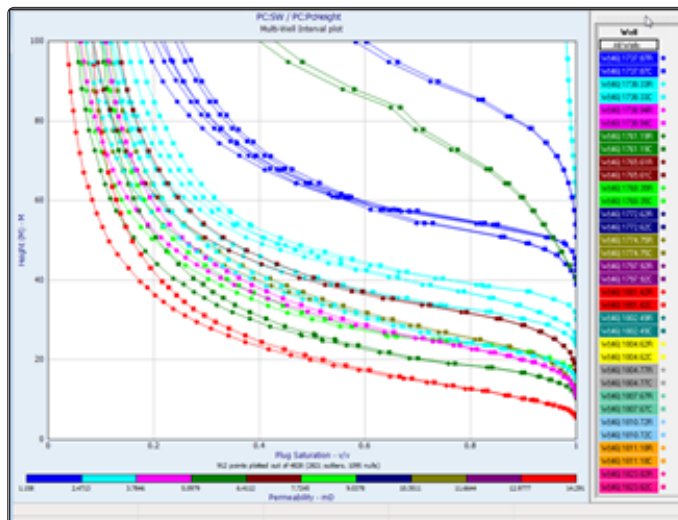


Figure 10: The results of experiments on capillary pressure on studied well of core samples. The minimum non-decreasing water saturation rate is based on these capillary pressure data is 20%

The fabric of porosity systems of the Chalky model, intercrystalline and untouched vuggy defined by Lønøy and Lucia. The studied facies are microscopic porosity, which is porosities in the form of equant pores with an average diameter of less than 1.16 mm. Micritic matrix is often developed in algae and muddy algal facies, facies with orbitolina dominated frequency and facies with an abundance of lithocodium algae in Shuaiba. The matrices have euhedral crystals of up to subhedral, micro-rhombus, with an average diameter of 5 microns. Among other factors, in addition to the presence of micritic texture, the processes of the pyritization to more than 10% in the samples of the studied formations, It is recognizable that it can be effective in reducing the specific resistivity. The study of clay minerals shows, the effect of minerals such as smectite and montmorillonite, but their role is not as high as those mentioned above and not in the studied reservoirs.

NMR answers

With the usual petrophysical investigations and reliance on conventional charts, the amount of high water saturation is calculated, which is due to the reduction of specific resistivity. Accordingly, in this study, the NMR nuclear magnetic resonance tool has been used to accurately determine the saturation of water for low specific resistance reservoirs using Variable T2 (relaxation time). The nuclear magnetization resonance directly measures the density of hydrogen nuclei in the reservoir fluid, since the density of the hydrogen nuclei in the water is clear, the data can directly represent the apparent porosity filled with water. The resonance of nuclear magnetism is related to the response of the atomic nucleus to magnetic fields. The magnetism generated by the rotation of atomic nuclei with the external magnetic field produces measurable signals. Based on the measurement of the nuclear magnetism, the pore size, fluid type, and porosity are measured. The experiments were carried out on 15 core specimens in the Air Brine and Oil brine tests of nuclear magnetic resonance to investigate the size of cavities containing oil and water fluids. Table 2 presents, the results of the analysis of nuclear magnetic resonance in the Oil Brine system in Shuaiba reservoir, reservoir fluids can be partially divided into the water of the clay, the water of moving water, gas, light oil and heavy oil. The distribution of cutoff behavior is determined on the basis of rocky species (Fig. 12). The average relaxation time for the rock is 1:15 milliseconds, the rock is 2: 50 milliseconds, the rock is 3: 70 milliseconds, the rock is 4: 300 milliseconds and the rock is 5:

20 milliseconds and rock are 6:90. The results of the analysis shown in table 2 of nuclear magnetic resonance in the Oil Brine system in Shuaiba reservoir. Table 2 illustrates variable T2 cutoff from 12 to 182 milliseconds for each rock types.

Table 2: The results of the analysis of nuclear magnetic resonance in the Oil Brine system in Shuaiba reservoir. In the table, the corresponding depths of the rock species, the variables of the cutoff T2, the logarithm of T2, the percentage of clay water porosity, the indispensable porosity of the water, Porosity of removable water, free fluid porosity, effective porosity, and absolute porosity, porosity of the laboratory and helium, permeability and saturation of non-reducing Sirr

Oil-Brine State															
S.No	Rock Type	Depth (M)	T2 Cutoff (msec)	T2 LM (msec)	MCBW (%)	MBVI (%)	MBFV (%)	MFFI (%)	MPHI (%)	MSIG (%)	QV (Frac)	Porosity (Weighting, %)	Porosity (He Phi, %)	Perm Kg(MD)	Sirr NMR (%)
NMR 1	1	1718.26	12.22	12.48	2.10	9.12	11.22	10.28	19.40	21.50	0.27	17.95	18.26	0.21	52.19
NMR 2	1	1726.77	17.78	18.25	1.30	7.93	7.92	6.98	13.60	14.90	0.24	13.04	14.23	0.13	53.14
NMR 3	2	1735.58	28.03	29.19	1.50	7.74	9.24	10.36	18.10	19.60	0.21	16.91	17.47	0.30	47.12
NMR 4	2	1742.96	20.04	23.15	2.30	7.42	9.72	15.08	22.50	24.80	0.26	20.64	20.97	0.30	39.18
NMR 5	1	1743.59	17.08	23.09	1.60	4.91	6.51	7.19	12.10	13.70	0.32	13.15	13.22	0.09	47.53
NMR 6	3	1755.39	62.23	68.88	1.90	7.99	9.89	18.31	26.30	28.20	0.19	24.65	25.43	1.75	35.06
NMR 7	2	1760.18	53.85	59.95	1.00	8.18	9.18	14.22	22.40	23.40	0.12	19.42	20.25	0.87	39.24
NMR 8	3	1761.77	61.90	71.05	2.50	5.63	8.13	13.17	18.80	21.30	0.32	17.92	17.59	0.86	38.19
NMR 9	5	1770.39	13.09	12.94	1.40	2.47	3.87	3.63	6.10	7.50	0.51	6.44	7.66	0.60	51.62
NMR 10	5	1774.62	10.25	6.32	2.40	3.22	5.62	1.78	5.00	7.40	0.89	5.17	4.82	0.17	75.93
NMR 11	3.00	1784.82	173.06	171.14	1.30	5.52	6.82	18.38	23.90	25.20	0.14	23.79	24.26	2.11	27.05
NMR 12	4	1785.47	182.94	208.65	1.10	7.01	8.11	20.29	27.30	28.40	0.11	25.19	27.79	13.71	28.56
NMR 13	4	1797.15	119.20	146.73	1.60	8.78	10.38	19.62	28.40	30.00	0.15	26.18	27.79	16.75	34.59
NMR 14	4	1801.66	105.69	102.28	1.50	7.41	8.91	19.79	27.20	28.70	0.14	25.14	28.83	2.67	31.03
NMR 15	5.00	1782.47	59.56	63.03	1.40	2.58	3.98	7.72	10.30	11.70	0.33	10.49	10.96	0.19	34.01

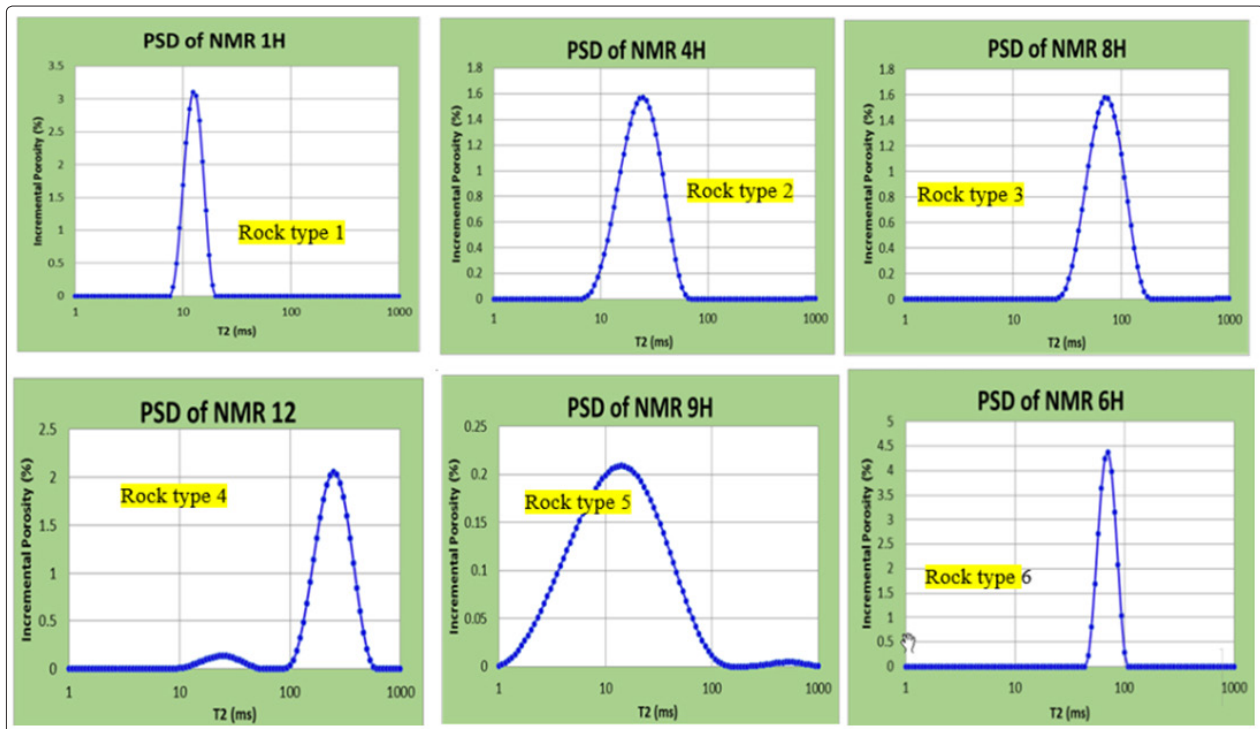


Figure 12: Determination of rock species of Shuaiba Formation, based on the distribution of pore size, behavior, shows NMR results.

For the Shuaiba Formation, the results of the T2 cutoff of the cores are used to determine the exact saturation of water. The values of the time of comfort are the supposed disconnection in the range of removable fluid hair and fluid, which varies between 12 and 170 milliseconds of microfacies with a low specific resistivity, and is suitable for microscopic porosity deposits. The study has shown that by decreasing the amount of comfort time for a given discontinuation, the amount of water saturation and vice versa increase with the increase in the amount of time the comfort of suppressing the amount of saturation is increased. The average of water saturation is calculated from the results of petro physical assessment and analysis of the graphs from nuclear magnetic resonance defines 50 % (Fig13).

Depth	GammaRay	Swi	Phi Bins	Comparison	NMR Phi	T2
DEPTH (M)	GKUT (api)	nmrSwiT (Dec)	nmrPhiB1 (Dec)	nmrPhie (Dec)	nmrPhiT (Dec)	SPECTA (mv)
	0. 100.	1. 0. 0.5	0.5 0. 0.5	0.5 0. 0.5	0.5 0. 0.5	0.3 3000
		nmrSw (Dec)	nmrPhiB2 (Dec)	nmrPhiT (Dec)	nmrBFT (Dec)	T2cutoff (mv)
		1. 0. 0.5	0.5 0. 0.5	0.5 0. 0.5	0.5 0. 0.5	0.3 3000.
		Sirr (%)	nmrPhiB3 (Dec)	nmrPhiT (Dec)	nmrCBW (Dec)	CBFT2cut (mv)
		100 0	0.5 0. 0.5	0.5 0. 0.5	0.5 0. 0.5	0.3 3000.
			nmrPhiB4 (Dec)			nmrT2M (ms)
			0.5 0. 0.5			0.3 3000.
			nmrPhiB5 (Dec)			
			0.5 0. 0.5			
			0.3 - 7ms			
			7 - 15ms			
			15 - 33ms			
			33 - 300ms			
			300 - 3000ms			
					Free Fluid	
					Capillary Water	
					Clay Water	

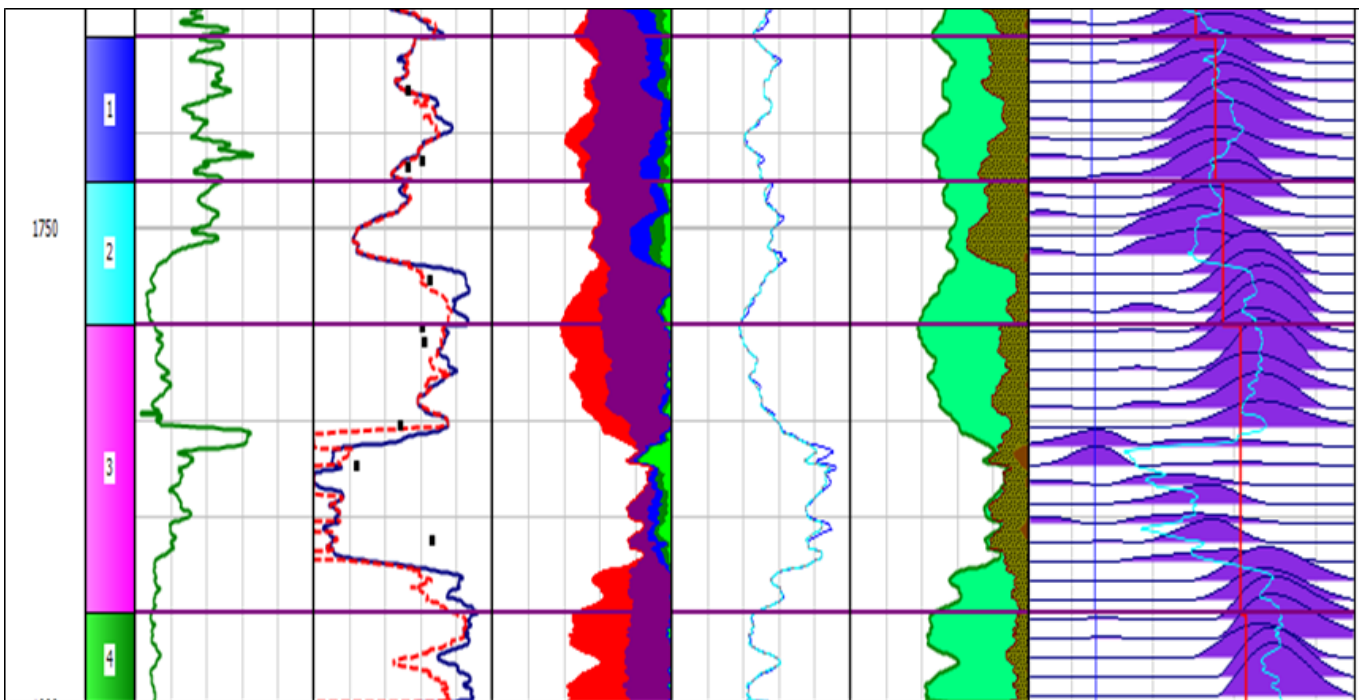


Figure 13: Combination between full set logs and NMR logs with NMR core results in Shuaiba formation. Water saturation varies between 35% to 50% results extract based on 15 core samples selected for NMR analysis in oil brine and air brine condition to get information about pore size clay bound water, moved oil and water and residual water saturation.

Conclusion

In general, the causes and factors which have led to the reduction of specific resistivity in the studied formations can be mentioned for the following reasons. Reducing the specific resistivity to texture changes and the presence of microscopic porosities in the deposits is not an increase in the displacement of water. The average radius of the diameter of pores is less than 3 microns. The matrices have euhedral to subhedral crystals, microcrystalline, with an average diameter of 5 microns. The microscopic porosities in the samples of the facies, the formations studied, are equant porosities with an average diameter less than 1.16 mm. In the dominant facade of the

lithocodium, which is the cortex, there is an incrustation activity that can produce their mercury buildings. Micritization and pyritization in the samples are the dominant diaphasic processes that can play a role in reducing the reading of the resistance chart. These diagenetic processes, as much as the presence of microscopic porosity, can reduce the strength of the main agent.

Based on microstructural analysis and fabrication of rocks of low-resistance hydrocarbon zones of Dariyan Formation in the eastern part of the Persian Gulf, 8 microfacies have been identified in the carbonate ramp section, which is classified in five rock categories,

and only in the class III Lucia (Mud dominated). The resistivity in the reservoir zones has also reached up to one-ohm meter, with microscopic porosities with radial dimensions of less than 3 microns. The processes of pyritization, micritization are also observed in facies, which can be effective in reducing specific resistivity. In microfacies such as Muddy Algal Bundstone facies, orbitolina facies, and facies with the frequency of lithocodium algae, a micritic matrix is found. The carbonate deposit of formation studied follow the defined models of Lønøy and Lucia, between porous microcrystalline porosity, Chalky, and Mudstone porosity models with microscopic porosity. In order to study the reservoir, the results of nuclear magnetic resonance intensification have been used on core samples and logs to determine the amount of water saturation. Based on the diverse distribution of pore size resulting from the results of the intensification of nuclear magnetism, six rock types can be identified that have average water saturation 50 % in the reservoir zone.

References

1. Lucia FJ (1995) Rock-fabric/petro physical classification of carbonate pore space for reservoir characterization: AAPG Bulletin 79: 1275-1300.
2. Granier B, Busnardo R (2003) New insight on the stratigraphy of the "Upper Thamama" in offshore Abu Dhabi, GeoArabia 56-73.
3. Winland D (2006) of Amoco, Carbonate Reservoir Characterization, Publication of articles in the paper journal "Oil and Gas Business" 206-217.
4. Buchem V, Maurer F (2010) Shuaiba Formation, Depositional Facies Distribution Revealed from Extended Reach Horizontal Wells in Al Shaheen Field, Offshore, Qatar. IPTC 55-64.
5. Al-Husseini MI (2007) Iran's crude oil reserves and production, Geo Arabia 12: 69-94.
6. Lønøy A, (2000) Making sense of carbonate pore system: AAPG Bulletin 90: 1381-1405.
7. Lucia FJ (1999) Carbonate reservoir characterization: Berlin, Springer-Verlag 226.
8. Dunham RJ (1962) Classification of carbonate rocks according to depositional texture In: Ham, W.E. Classification of carbonate rocks. American Association of Petroleum Geologists Memoir 1: 108-121.
9. Amafule JO, Altunbay M, Tiab D, Kersey DG, Keelan DR (1993) Enhanced reservoir description: Using core and log data to identify hydraulic (flow) units and predict permeability in uncored intervals/wells. Proceedings of the 68th SPE Annual Technical Conference and Exhibition, October 3-6, 1993, Houston, Texas, Society of Petroleum Engineers 205-220.
10. Bathurst RGC (1976) Carbonate sediments and their diagenesis chapter 12: Neomorphic processes in diagenesis. Elsevier Pub 475-516.
11. Burchette TP & Wright VP (1992) Carbonate ramp depositional system, Sedimentary Geology 79: 3-57.
12. Cantarero I, Travé A (2014) Diagenesis Impact on Permeability of a Large Carbonate Reservoir, AAPG International Conference & Exhibition, Istanbul, Turkey 14-17.
13. Flugel E, (2004) Microfacies of carbonate rocks. Berlin, Springer 976.
14. Lucia FJ (1983) Petro physical parameters estimated from visual descriptions of carbonate rocks: A field classification of carbonate pore space: Journal of Petroleum Technology 216: 221-224.
15. Lucia FJJ, Jennings W, Ruppel SC (2004) a, South Wasson Clear Fork reservoir modelling: The rock fabric method for constructing flow layers for fluid flow simulation (abs.): AAPG Hedberg Research Conference, March 15-18, 2004, El Paso,
16. Tucker ME, Wright PV (1996) Carbonate Sedimentology, Black Scientific Pub 482.
17. Tucker ME (2001) Sedimentary Petrology, Black Scientific Pub 260.
18. Wilson BR (1975) Carbonate Facies in Geological History. Springer, Berlin 471.

Copyright: ©2018 Bita Arbab. This is an open-access article distributed under the terms of the Creative Commons Attribution License, which permits unrestricted use, distribution, and reproduction in any medium, provided the original author and source are credited.